J. Plasma Fusion Res. SERIES, Vol. 5 (2002) 238–241

Confinement Characteristics of Low Density FRC Plasma

KODERA Fuji, ASAI Tomohiko, OKUBO Mamoru, OKADA Shigefumi and GOTO Seiichi
Plasma Physics Laboratory, Graduate School of Engineering, Osaka University, Suita 565-0871, Japan

(Received: 11 December 2001 / Accepted: 17 June 2002)

Abstract

A new ionization process of the working gas through the fast neutral particles is utilized in order to assist in the formation of the field reversed configuration plasma. This method improves the lower density limit of the formed plasma. Characteristics of the field reversed configuration plasma are investigated in the low density region of the order of 1×10^{20} m^{-3} for the fusion plasma core. The particle confinement time τ_N is larger than the expected value of the coefficient from the empirical scaling by a factor of 2.8. It is found that the flux decay time τ_ϕ and the energy decay time τ_E are obtained to be $\tau_\phi = 0.89\tau_N$ and $\tau_E = 0.41\tau_N$, respectively, in the low density region.

Keywords:

field reversed configuration, low density formation, neutral beam ionization, confinement scaling, rotational instability

1. Introduction

A field reversed configuration (FRC) plasma [1] is an elongated high β compact toroid without toroidal field, which is proposed as a candidate for a D-^{3}He fusion reactor core. The conceptual reactor design 'ARTEMIS' [2] has been proposed based on the FRC plasma. This design requests the plasma parameters of the electron density $n_e \sim 4 \times 10^{20}$ m^{-3} in the initial formation before the main heating with high power neutral beams. Characteristics of the FRC plasma should be then explored in the low density region of the order of 1×10^{20} m^{-3}. The improvement of the formation method is required in order to attain the low density FRC plasma. The density lower than 1×10^{20} m^{-3} might be realized by decreasing the filling pressure if the sufficient pre-ionization can be taken. However there exists a lower limit of the formed density in usual experimental conditions as for the initial breakdown of the working gas. A pre-ionization process of the working gas of the deuterium is utilized in order to assist the ionization process through the neutral beam injection. The free electron increment in the gas is due to the ionization process between the injected high energy neutrals of the hydrogen and gaseous molecule. This method improves the lower limit of the formed FRC plasma density [3]. This method enables the density limit to be lowered, and characteristics of the FRC plasma are investigated in the low density region of the order of 1×10^{20} m^{-3}.

2. Instrumentation

A schematic diagram of the FRC Injection experiment (FIX) device [4] is shown in Fig. 1(a). This device has a formation region and a confinement region. The formation region shown in Fig. 1(b) consists of a 2120 mm-long quartz tube with a 275 mm inner diameter and a 309 mm inner diameter theta-pinch coil. The theta-pinch coil is composed of 14 coils with 76 mm widths in each with its separation 8 mm. The position $z = 0$ indicates the center of the coil axis, and this area is called the midplane. A pair of driven mirror coils, named mirror left (ML) and mirror right (MR), is mounted 50 mm apart from each end of the theta-pinch

Corresponding author's e-mail: kodera@ppl.eng.osaka-u.ac.jp

coil. They have the same inner diameter as the theta-pinch coil.

The FRC plasma is produced by the theta pinch method. The fast rising (3.5 μs) magnetic field B_e is applied to preheated plasma, and the FRC plasma is formed. The peak value of B_e can be chosen to be from 0.40 T to 0.85 T. Usually, the discharge current is crowbarred at its peak, but in this experiment its timing is changed to the value shorter than the normal condition to produce weaker B_e keeping the same rising rate dB_e/dt unchanged. It is found that the weaker peak field is necessary to avoid a collapse of the compressed plasma during the pinch phase.

The formed FRC plasma can be quickly translated to the confinement region through the proper control of the ML and the MR coils. In the right-hand side of Fig. 1(a), the high power ion beam source is shown, which is utilized for our low density formation experiment. The reason why this is mounted so far from the formation region is to avoid ion source electrodes damage by the end-loss plasma effect, and also to keep the compatibility with the translation experiment.

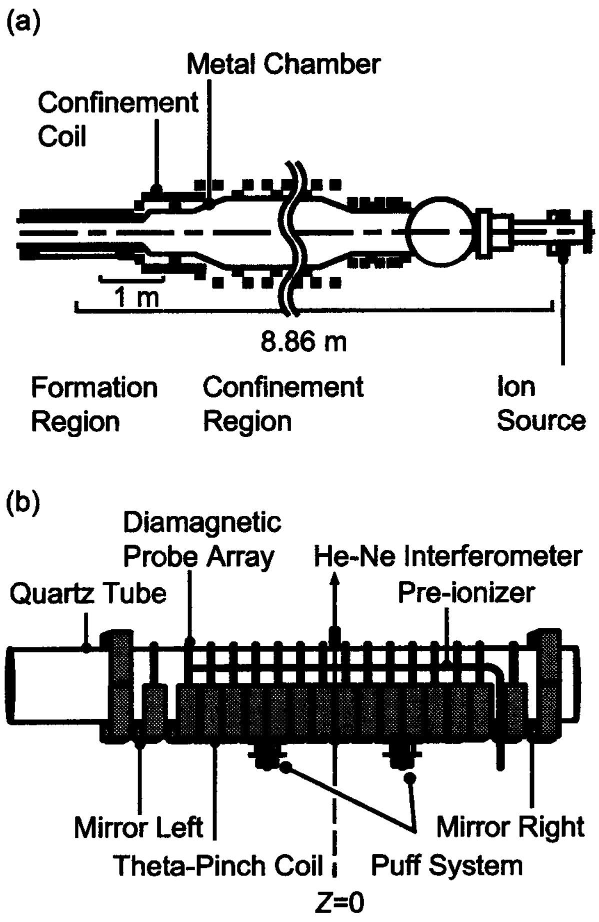

Fig. 1 FIX device

Our beam system employs the bucket type ion source [5,6]. The axis of the ion source coincides with the geometrical axis of the FIX device in order to aim at the formation region. The electrode has a racetrack shape and the effective length, the minor width and the thickness of copper electrodes are 306 mm, 151 mm and 1.5 mm, respectively. The electrode has 1757 small holes of 4 mm and 4.5 mm in diameter.

The plasma diagnostics consist of a diamagnetic loop array around the formation tube and an interferometer. Each loop has its own compensation probe. The separatrix radius r_s is derived from each loop signal and the axial r_s profile is estimated from 11 loop signals. A line integrated density $\int n_e dr$ is measured with a 3.39 μm He-Ne laser interferometer at the midplane.

The filling pressure in the quartz tube governs the plasma density of the formed FRC. It is fairly difficult to measure the filling pressure in our case, because the working gas is filled into the vacuum vessel by means of the puff system. The decompressed plasma in the pre-heating (PH) phase is utilized in order to indicate the equivalent filling pressure. When the plasma produced by the PH alternating current expands to reach the wall in the first quarter period, it is assumed that the neutral gas is fully ionized and the particle diffusion can be neglected in the axial direction. We can then define the initial plasma density $\langle n_{e0} \rangle = \int n_e dr / 2r_t$ and the molecule number density $n_{D2} = \langle n_{e0} \rangle / 2$, where r_t is the quartz tube radius.

3. Experimental Results

In order to overcome the pre-ionization problem, a powerful neutral beam has been employed as the pre-pre-ionizer. The neutral beam is injected into the vacuum vessel from $t = -3$ ms and the typical power measured in the ion source is 440 kW (23 kV, 19 A). The typical time evolution of the line integrated density of the plasma in the range more than 1.0×10^{21} m^{-3} is shown in Fig. 2, where the time is measured from the start of the PH field. The molecule number density is $n_{D2} \cong 1.6 \times 10^{20}$ m^{-3} which corresponds to an equivalent filling pressure of 610 mPa. The FRC plasma is formed and reaches a quiescent phase after a radial and axial compression motion. The characteristic parameters in the quiescent phase are obtained as an average value between $t = 25.0$ μs and $t = 27.5$ μs. The FRC plasma density is 5.1×10^{21} m^{-3} in the quiescent phase. The line integrated density is rapidly decayed after the formation.

The n = 2 rotational instability appears at 42 μs, its period is about 4.8 μs, and the FRC configuration disappears at $t \cong 100$ μs.

A density lower than 1.0×10^{21} m^{-3} is formed by decreasing the filling pressure. The waveform of the line integrated density is shown in Fig. 3 at the reduced $n_{D2} \cong 2.0 \times 10^{19}$ m^{-3}. The density is 5.0×10^{20} m^{-3} in the quiescent phase. The line integrated density has a gentle decay before the n = 2 rotational instability starts. The ripple-like oscillation of the waveform in Fig. 3 begins from $t \cong 33$ μs with the period shorter than that in other case. In this case, the instability does not grow and disappears at $t \cong 55$ μs. It is found that this configuration is sustained after the excitation of the instability.

As presented in Fig. 3, the formed FRC plasma assisted by the neutral beam does not have the indication that the configuration disappears due to n = 2 rotational instability. The particle confinement time τ_N is derived from the waveforms of the diamagnetic probe

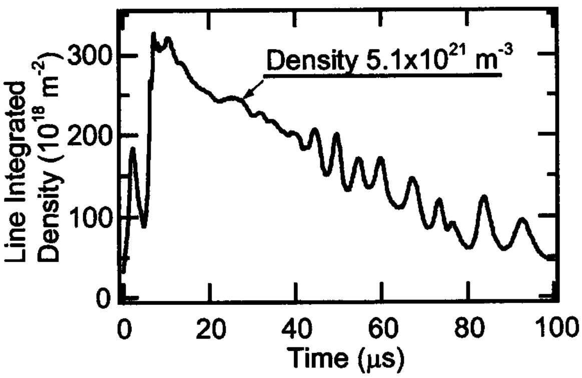

Fig. 2 The line integrated density of the plasma in the range more than 1.0×10^{21} m^{-3}.

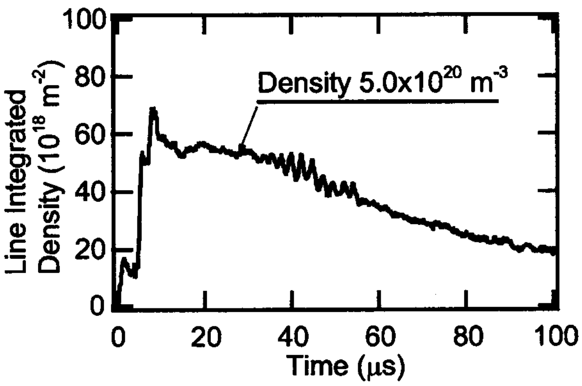

Fig. 3 The line integrated density of a low density plasma less than 1.0×10^{21} m^{-3}.

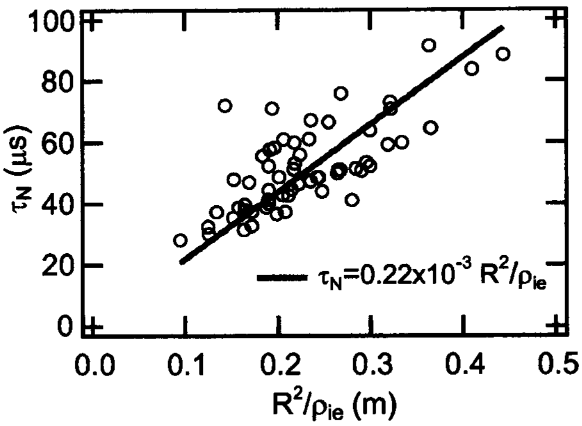

Fig. 4 Relation of the particle confinement time τ_N and R^2/ρ_{ie}. The solid line is the fitting line for all data.

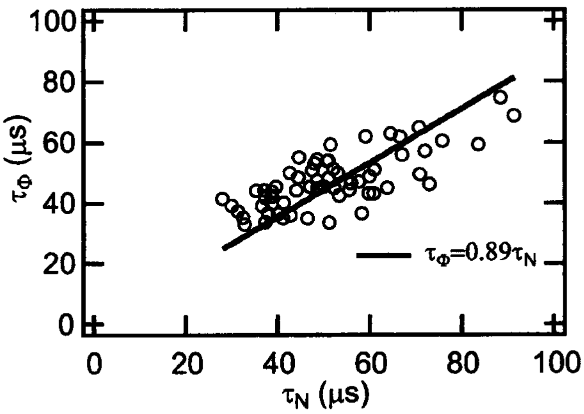

Fig. 5 Relation of the flux decay time τ_ϕ and the particle confinement time τ_N. The solid line is the fitting line for all data.

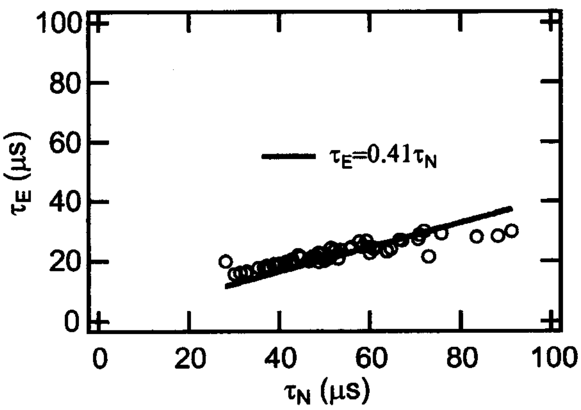

Fig. 6 Relation of the energy decay time τ_E and the particle confinement time τ_N. The solid line is the fitting line for all data.

array and the interferometer during the whole time of the configuration life. The confinement time can be obtained by an exponential fitting curve to the time evolution of the particle inventory. The confinement times of the low density plasmas of 61 shots are plotted versus R^2/ρ_{ie} in Fig. 4, where R and ρ_{ie} are the radius of the magnetic field null ($r_s/\sqrt{2}$) and the ion gyro radius in the external field, respectively. The solid straight line represents a line fit $\tau_N = 0.22 \times 10^{-3}R^2/\rho_{ie}$ to the experimental data, where the ion temperature is taken to be two thirds of the total temperature. It is mentioned that τ_N is larger than the expected value of the coefficient from the empirical scaling by a factor of 2.8 [7]. The difference might be explained from the small s value ($\cong \int_R^{r_s} r\mathrm{d}r/r_s\rho_i$, ρ_i is ion gyro radius). As the s value increases, the confinement time is usually improved. When the s value is small, the confinement time becomes longer than the estimated value due to the effect of the edge layer plasma [8]. As the value of s is between 0.2 and 0.9 in the low density regime in our case, the confinement time might be longer than the expected value from the scaling.

The flux decay time τ_ϕ and the energy decay time τ_E are compared to τ_N in order to study the characteristics of the FRC plasma in the low density regime. The flux decay time can be obtained from an exponential fitting curve to the time evolution of the trapped flux, too. The data points of the flux decay time are shown in Fig. 5. The solid straight line indicates a line fit $\tau_\phi = 0.89\tau_N$ to the experimental data. It is found that τ_ϕ is nearly equal to τ_N. The energy decay time τ_E can be estimated from $1/\tau_E \cong 5/3\cdot 1/\tau_V + 1/\tau_{pm}$, where τ_V and τ_{pm} are the volume and $P_m (= B_e^2/2\mu_0)$ decay times, respectively [9]. However, the effect of the length change can be ignored because the 70 % or more data indicated in 61 shots of Fig. 6 shows over $l(t_e)/l_0 = 0.7$ at the e-folding time t_e of the volume decay. Here, l_0 is the initial length and $l(t_e)$ is the length of $t = t_e$. The obtained result is shown in Fig. 6. The solid straight line represents a line fit $\tau_E = 0.41\tau_N$ to the experimental data. It is found that τ_E is about half value of τ_N. This result indicates that the energy decay time is more influenced by the decay rate of the magnetic field as presented in the relation above. When the magnetic field will be raised up, this decay time must be prolonged, too.

4. Summary

An ionization process of the working gas through the fast neutral particles is utilized in order to assist in the formation of the FRC plasma. Characteristics of the FRC plasma are explored in the low density region of the order of 1×10^{20} m^{-3}. The $n = 2$ rotational instability does not grow up to the broken state of the FRC. The reason for this phenomenon has not been explained so far. The particle confinement time τ_N is larger than the expected value of the coefficient from the empirical scaling by a factor of 2.8. It is found that the flux decay τ_ϕ and the energy decay time τ_E are obtained to be $\tau_\phi = 0.89\tau_N$ and $\tau_E = 0.41\tau_N$. This relationship holds against the all data including the shots in case of the occurrence of the $n = 2$ instability, since the configuration itself can be kept for the case.

References

[1] M. Tuszewski, Nucl. Fusion **28**, 2033 (1988).
[2] H. Momota *et al.*, Fusion Technol. **21**, 2307 (1992).
[3] F. Kodera *et al.*, J. Plasma and Fusion Res. **77**, 1145 (2001).
[4] T. Asai *et al.*, Phys. Plasmas **6**, 2294 (2000).
[5] Y. Ueda *et al.*, Rev. Sci. Instrum. **65**, 2587 (1994).
[6] F. Kodera *et al.*, J. High Temp. Soc. **25**, 318 (1999).
[7] K.F. McKenna *et al.*, Phys. Rev. Lett. **50**, 1787 (1983).
[8] J.T. Slough *et al.*, Phys. Plasmas **2**, 2286 (1995).
[9] A. L. Hoffman *et al.*, Nucl. Fusion **33**, 27 (1993).